Cosmological simulations of galaxy formation

Andreas
Pawlik
(MPA)

Cosmological simulations allow us to follow the evolution of matter - both dark matter and baryons - in the expanding Universe accurately to the nonlinear regime of high densities that is typically not analytically accessible.

In this lecture I will review some of the main computational techniques employed to perform cosmological simulations. Excellent reviews of the subject can be found in Dolag et al. (2008) and Springel (2010), just to name a few. Accessible introductions to the theory of hierarchical structure formation in the ΛCDM Universe that I will adopt as framework are in the text books of Padmanabhan (1993) and Mo, van den Bosch, White (2010).

The lecture consists of 3 parts, in which I discuss techniques (I) to simulate Cold Dark Matter, (II) to generate initial conditions, and (III) to follow the dynamics of the gas and the assembly of galaxies.

(I) Dark matter

The evolution of the phase space density f of dark matter is assumed to obey the collisionless Boltzmann equation (CBE):

$$\frac{df}{dt} = \frac{\partial f}{\partial t} + \vec{v} \frac{\partial f}{\partial \vec{r}} - \frac{\partial \varphi}{\partial \vec{r}} \frac{\partial f}{\partial \vec{v}} = 0 ,$$

where the gravitational potential φ is given by

$$\nabla^2 \varphi(\vec{r}, t) = 4\pi G \int f(\vec{r}, \vec{v}, t) \, d\vec{v} .$$
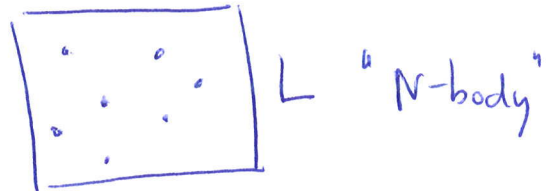
(e.g., Mo, van den Bosch, White 2010)

①

⑩ N-body approach

The most common approach to solving the CBE is by representing the dark matter fluid by N particles inside a box of size L. The dynamics of the particles is determined by the characteristic equations of the CBE (e.g., Springel et al. 2001):

$$\dot{\vec{v}} = -\nabla \phi \qquad \text{(Eq. 1)}$$
$$\dot{\vec{r}} = \vec{v} \qquad \text{(Eq. 2)}$$
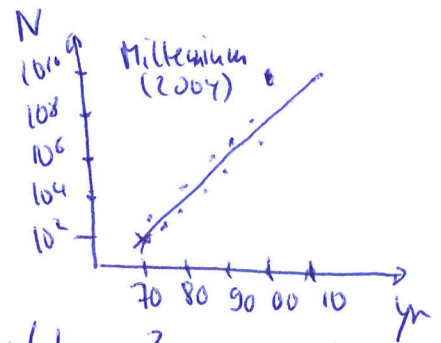$$\nabla^2 \phi = 4\pi G \rho(\vec{r}, t) \qquad \text{(Eq. 3)}$$

L "N-body"

Notes:

First N-body simulations: 1960's/70's, ~100 particles
(e.g., Aarseth 1963, Peebles 1970, Press & Schechter 1974)

Today: simulations with $10^{10} - 10^{11}$ particles exist (e.g., "Bolshoi", Klypin et al.; "Horizon", Teyssier et al.; "Millennium", Springel et al.)

This means that N-body simulations have doubled their size every 16-17 months.
Note that Moore's law states that computers double their speed every 18 months.

Question: What have we learned from these simulations?

①.2 Comoving Coordinates

It is useful to divide out the cosmological expansion of the Universe by introducing comoving coordinates $\vec{r}'$ with

$$\vec{r}' = \vec{r}/a, \quad \vec{v}' = \dot{\vec{r}}', \quad \nabla' = a\nabla,$$

where $a(t)$ is the expansion factor. Then, Eq. 1 becomes

$$\dot{\vec{v}} = \ddot{\vec{r}}'a + \dot{a}\dot{\vec{r}}' + \ddot{a}\vec{r}' + \dot{a}\dot{\vec{r}}' = -\nabla\phi$$

$$\xrightarrow{\vec{v}' = \dot{\vec{r}}'} a\dot{\vec{v}}' + 2\dot{a}\vec{v}' + \ddot{a}\vec{r}' = -\nabla\phi$$

$\nabla q = a^{-1} \nabla \phi$
$\nabla'_i r^2 = \vec{r}'$

$$\boxed{\dot{\vec{v}}' + 2H \vec{v}' = -\frac{1}{a^3} \nabla' \phi'} , \qquad (Eq\ 4)$$

where $H = \frac{\dot{a}}{a}$ (Hubble "constant") and $\phi' = a\phi + \frac{a^2 \ddot{a}}{2} r'^2$

(peculiar potential)

Also, applying ∇^2 to ϕ':

$$a \nabla^2 \phi = \nabla^2 \phi' - \frac{a^2 \ddot{a}}{2} \nabla^2 \vec{r}'^2$$

$\nabla^2 \phi = 4\pi G \rho$

$\Longrightarrow$

$\nabla^2 = a^{-2} \nabla'^2$

$$a \, 4\pi G \rho = a^{-2} \nabla'^2 \phi' - \frac{a^2 \ddot{a}}{2} a^{-2} \nabla'^2 \vec{r}'^2$$

$\nabla'^2_{\frac{1}{2} r'^2} = 3$

$$= a^{-2} \nabla'^2 \phi' - 3\ddot{a}$$

$$\Rightarrow \boxed{\nabla'^2 \phi' = a^3 \, 4\pi G \, \rho + 3a^2 \ddot{a}} \qquad (Eq\ 5)$$

To solve the set of equations 4 & 5, we need to specify:
- the evolution of $a(t)$, the expansion factor
- the gravitational potential ϕ
- a time-integration scheme
- initial conditions

Ⅱ.3) The expansion factor $a(t)$

The evolution of the expansion factor follows directly from the assumption of a homogeneous and isotropic universe in General Relativity (plug Friedman-Robertson-Walker metric into Einstein's equation of gravity).

An approximate Newtonian treatment (assuming non-relativistic matter and ignoring the cosmological constant) is as follows. In a spherically symmetric system, the gravitational force at radius r has only contributions from the mass interior to it, acting as if the mass were concentrated in a point at $r=0$ (Newton's theorem).

3

Hence, mass elements i move according to

$$\ddot{r}_i(t) = \frac{4}{3}\pi r_i^3 \bar{\varrho} \, \frac{G}{r_i^2}$$

$$= -\frac{4}{3}\pi G \bar{\varrho} \, r_i(t)$$

Division by $r_i(0)$ then yields

$$\ddot{a}(t) = -\frac{4}{3}\pi G \bar{\varrho}(t) \, a(t)$$

$$\Rightarrow \boxed{\ddot{a}(t) = -\frac{4}{3}\pi G \frac{\bar{\varrho}_0}{a^2(t)}} \quad , \quad \bar{\varrho}_0 = a^3 \bar{\varrho} \quad \text{(comoving mean density)}$$

Multiplication with $2\dot{a}$ and integration yields

$$\frac{d}{dt}\left[\dot{a}^2 - \frac{8}{3}\pi \frac{G\bar{\varrho}_0}{a(t)}\right] = 0$$

$$\boxed{\dot{a}^2 - \frac{8}{3}\pi \frac{G\bar{\varrho}_0}{a(t)} = -k}$$

Friedmann equations

(in General Relativity, k is the curvature of space)

Note: $\nabla'^2\phi' = a^3 \, 4\pi G \varrho + 3a^2\ddot{a} \Rightarrow \nabla'^2\phi' = 4\pi G \,(\varrho' - \bar{\varrho})$

$\Rightarrow$ gravitational potential is sourced by density fluctuations

(a fully general relativistic treatment gives the same results)

(I.4) Computing the gravitational potential ϕ

(a) Direct summation (Particle-Particle, "PP")

$$\phi(\vec{r}) = -G \sum_j \frac{m_j}{\left(|\vec{r}-\vec{r}_j|^2 + \varepsilon^2\right)^{1/2}}$$

ε: Scale on which forces are softened. This reduces the spurious two-body relaxation effects that occur if the collisionless fluid is not sampled with sufficiently many particles (e.g., Springel et al. 2001)
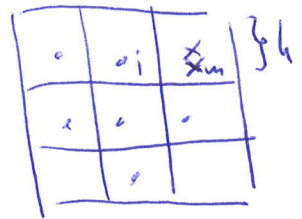
Advantages: simple, accurate

Disadvantages: computation time $\propto N^2 \Rightarrow$ rarely in use (but see GRAPE (GPU, e.g., Steinmetz 1996)

(4)

(b) Particle-Mesh ("PM")

Idea: Solve the gravitational potential on a mesh

$$\phi(\vec{r}) = \int \rho(\vec{r}') \, g(\vec{r}-\vec{r}') \, d^3r'$$

$$g(\vec{r}) = -\frac{G}{|\vec{r}|} \quad : \quad \text{Green's function}$$

In Fourier space, the convolution is a simple multiplication:

$$\hat{\phi}(\vec{u}) = \hat{\rho}(\vec{u}) \, \hat{g}(\vec{u}) \quad \leftarrow \text{needs to be computed only once}$$

Density assignment (e.g., Hockney & Eastwood 1988)

Give particles i shape $S(\vec{x})$ within which the mass is spread out. To each mesh cell, assign the fraction of mass in that cell:

$$W(\vec{x}_n - \vec{x}_i) = \int_{\vec{x}_n - h}^{\vec{x}_n + h} S(\vec{x}' - \vec{x}_i) \, d\vec{x}' = \int \Pi\left(\frac{\vec{x}' - \vec{x}_n}{h}\right) S(\vec{x}' - \vec{x}_i) \, d\vec{x}'$$
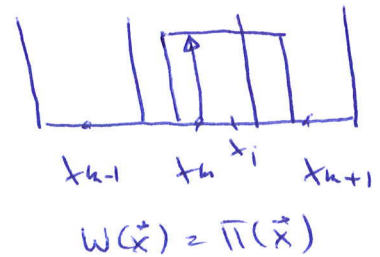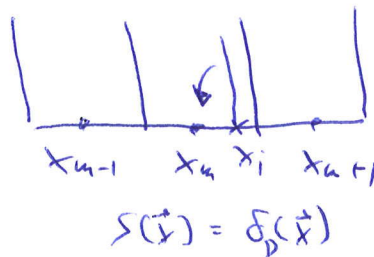
center of mesh cell

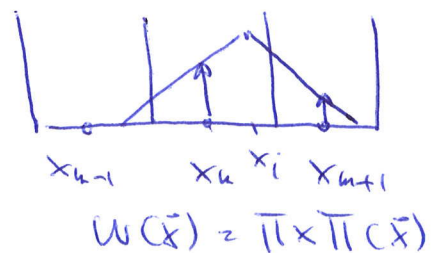$$\text{when } \Pi(\vec{x}) = \begin{cases} 1, & |\vec{x}| \leq \frac{1}{2} \\ 0, & \text{otherwise} \end{cases}$$

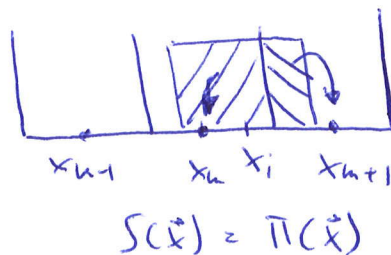$$\Rightarrow \rho(x_n) = \frac{1}{h^3} \sum_{i=1}^{N} m_i \, W(\vec{x}_i - \vec{x}_n)$$

$\Rightarrow$ A hierarchy of shapes is in use:

NGP
(Nearest Grid
Point)

$x_{n-1} \quad x_n \; x_i \quad x_{n+1}$

$$S(\vec{x}) = \delta_D(\vec{x})$$

$x_{n-1} \quad x_n \; {}^{x_i} \quad x_{n+1}$

$$W(\vec{x}) = \Pi(\vec{x})$$

CIC
(Clouds In Cells)

$x_{n-1} \quad x_n \; x_i \quad x_{n+1}$

$$S(\vec{x}) = \Pi(\vec{x})$$

$x_{n-1} \quad x_n \; x_i \quad x_{n+1}$

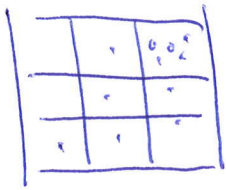$$W(\vec{x}) = \Pi \times \Pi(\vec{x})$$

TSC
(Triangular Shaped
Clouds)
⋮

Advantages: accurate, computation time $\propto N + N_g \log N_g$

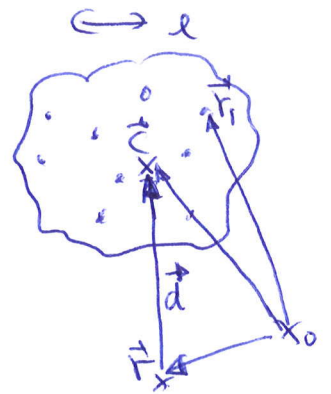Disadvantages: • grid can introduce force errors that are anisotropic on the scale of mesh cells

• Dynamic range limited by N_g, which is limited by memory. However, N-body particles are often highly clustered.

→ Dynamic range can be extended using an adaptive mesh ("APM", e.g., Couchman et al. 1995)

(c) Tree

Idea: multipole expansion of the gravitational potential around center of mass $\vec{c}$

$$\phi(\vec{r}) = -G \sum \frac{m_i}{|\vec{r} - \vec{r}_i|}$$

$$\frac{1}{|\vec{r} - \vec{r}_i|} = \frac{1}{|(\vec{r} - \vec{c}) - (\vec{r}_i - \vec{c})|} \quad , \quad \vec{d} = \vec{r} - \vec{c}$$

$$= \frac{1}{|\vec{d} + \vec{c} - \vec{r}_i|} \overset{|\vec{r}_i - \vec{c}| \ll |\vec{d}|}{=} \frac{1}{|\vec{y}|} - \overset{\smile}{y} \frac{(\vec{c} - \vec{x}_i)}{|\vec{y}|^3} + \cdots$$
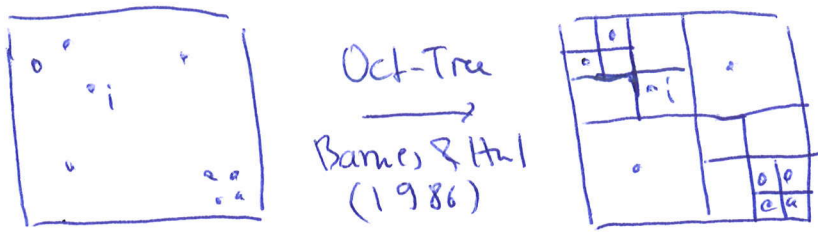
monopole

dipole: vanishes when summed over all particles in the group
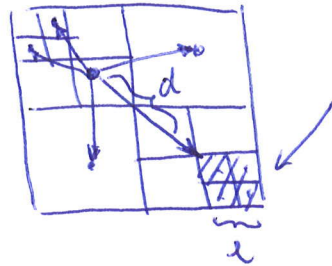
⇒ Stop following individual particles and instead use monopole (+ quadrupole + ...) of the particle group IF group size is small in comparison with distance $|\vec{d}|$:

$$|\vec{d}| > \frac{\ell}{\theta} \quad , \quad \text{where the opening angle } \theta \text{ controls the force accuracy}$$

In practice, particles are grouped in a tree (Barnes & Hut 1986; also, Springel et al 2001).

Oct-Tree
$\xrightarrow{}$
Barnes & Hut
(1986)

Example: gravitational force on particle i:

tree node is not opened because
$$d > \frac{\ell}{\theta}$$
i.e., 4 particles are replaced by 1 monopole

Advantage: Typical computation time $\propto N \log N$
(Disadvantage: accuracy depends on θ)

(d) Hybrid methods

The techniques above are often combined using a force split
(e.g., Springel 2005, "Tree-PM"):

$$\phi_k^{long} = \phi_k \exp(-\vec{k}^2 r_s^2)$$

→ long-range force computed on Fourier mesh using PM

→ if r_s is chosen slightly larger than the mesh cell size, force anisotropies are avoided

$$\phi_k^{short} = \phi_k \left\{ 1 - \exp[-\vec{k}^2 r_s^2] \right\}$$

→ short-range force is computed in real space using Tree/PP after Fourier transform:
$$\phi(r) = -\frac{Gm}{r} \, erfc\left(\frac{r}{2 r_s}\right)$$
(single particle)

⇒ Tree/PP computation is local

Advantage: combines speed and accuracy of PM with adaptivity of Tree/PP

(I.5) Time Integration (e.g., Power et al 2003; Springel 2005)

Advance solution of the ordinary differential equations of form
$\dot{y} = f(y)$ in discrete time steps of size Δt.

Example: $y_{n+1} = y_n + f(y_n) \Delta t$ ("Euler" scheme)

Note: The Euler scheme does a poor job in conserving the energy of the integrated system, and is therefore not used. Instead: Leap-frog integrator (Springel 2005)

Time step: $\Delta t \sim t_{dyn} \sim \frac{1}{\sqrt{G\rho}}$

However, ρ is not readily accessible in the simulation. A simple alternative is
$$\Delta t = \alpha \sqrt{\frac{2\epsilon}{|\vec{a}|}} \quad , \text{where}$$
ϵ is the force softening scale, $\vec{a}$ the acceleration and α a numerical parameter to control the integration accuracy.

Note: In cosmological simulations, because of the large dynamic range in $\vec{a}, \vec{f}$, each particle is integrated with its own individual time step Δt_i.

(II) Initial Conditions (e.g., Sirko 2005)

Generation of initial conditions proceeds in 3 steps:
(1) Definition of the initial density field
(2) Generation of a uniform distribution of particles to represent the unperturbed Universe
(3) Displacement of the particles to generate the desired density field

(II.1) The initial density field

$$\vec{\rho}(\vec{x}) = (1 + \delta(\vec{x})) \bar{\rho}$$
$$\delta_{\vec{k}} \equiv \hat{\delta}(\vec{k}) = \int \delta(\vec{x}) e^{-i\vec{k}\vec{x}} d\vec{x}$$

⑧

Assumption ("Cosmological Statistical Principle"): At sufficiently early times, the real and imaginary parts of $\delta_k = a_k + i b_k$ are independent Gaussian random variables with zero mean and variance μ_k^2, i.e.,

$$P(a_k, b_k)\, da_k\, db_k = \frac{1}{2\pi \mu_k^2} \exp\left\{ -\frac{a_k^2 + b_k^2}{2\mu_k^2} \right\} da_k\, db_k$$

Note: $\delta(\vec{x}) = \int \hat{\delta}(\vec{k})\, e^{i \vec{k}\vec{x}}\, d\vec{k}$ is then also Gaussian.

Let's write $\delta_k = A_k\, e^{i\theta_k}$. Then

$$P(A_k, \theta_k)\, dA_k\, d\theta_k = \frac{1}{2\pi} \frac{A_k}{\mu_k^2} \exp\left\{ -\frac{1}{2} \frac{A_k^2}{\mu_k^2} \right\} dA_k\, d\theta_k$$

→ phase θ_k is uniformly distributed in $(0, 2\pi)$
→ Amplitude A_k is Rayleigh-distributed

A Rayleigh random variable can be generated from a uniform random variable $u_{A_k} \in (0,1)$ using $A_k = \sqrt{-2\mu_k^2 \ln u_{A_k}}$

$$\Rightarrow \delta_k = \sqrt{-2\mu_k^2 \ln u_{A_k}}\; e^{i u_{\theta_k}}\,, \quad u_{\theta_k} \text{ random in } (0, 2\pi)$$

Power spectrum $P(k) \equiv \langle |\delta_k|^2 \rangle = \frac{\mu_k^2}{2}$

$$\Rightarrow \boxed{\; \delta_k = \sqrt{-P(k) \ln u_{A_k}}\; e^{i k u_{\theta_k}} \;} \quad \begin{array}{l} \text{initial density} \\ \text{field (on grid)} \end{array}$$

The Power spectrum $P(k)$:

In linear theory, density fluctuations at different wavenumber k grow independent of each other (no "mode-mixing"). It is common to write

$$\hat{\delta}(\vec{k}, a) = \hat{\delta}(\vec{k}, a_i)\; T(k, a_m) \frac{D(a)}{D(a_m)}\,, \quad \text{where}$$

$T(k, a_m)$: linear theory transfer function that relates fluctuations in the post-recombination matter-dominated era a_m to the initial fluctuations at a_i
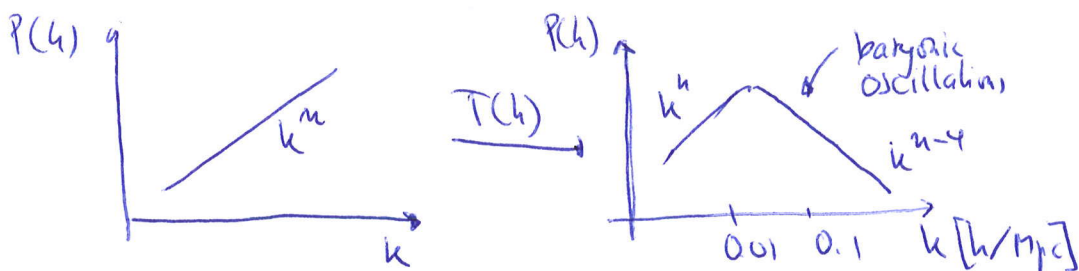
(9)

$D(a)$: linear theory growth factor that describes the (wave length - independent) growth of fluctuations in the post-recombination era (e.g., Mo, van den Bosch, White 2010).

The power spectrum is then
$$P(k,a) = P(k, a_i) \, T^2(k, a_m) \, \frac{D^2(a)}{D^2(a_m)}$$

Theory (inflation) predicts
$$P(k, a_i) \propto A k^n \qquad , \; n \simeq 1$$

The linear theory transfer function can be accurately computed (using codes like CMBFast, Seljak & Zaldarriaga 1996)

Note 1: The kink in the post-recombination power spectrum arises because sub-horizon fluctuations grow at different rates during the radiation- and matter-dominated epochs

Note 2: At high k, structure formation proceeds hierarchically:
$$\sigma^2 \equiv \int P(k) k^2 \, dk = \int P(k) k^3 \, d\ln k$$

variance of density fluctuations

contribution per decade

$$P(k) = k^{n-4} \Rightarrow P(k) k^3 = k^{n-1} \overset{n=1}{=} \text{const.}$$

$\Rightarrow$ The smallest-scale fluctuations collapse simultaneously.

Note 3 :   Current theories do not predict the normalization
of the power spectrum. It is usually normalized by
requiring

$$\sigma_8 \simeq 1 \quad \text{(as observed)}, \quad \text{where}$$

$$\sigma_R^2 = \int P(k)\, \hat{W}_R^2(k)\, d^3k$$

is the variance of the linearly extrapolated (to $z=0$)
density field averaged in spheres of radius, $R\,[h/Mpc]$,
and $\hat{W}_R(k)$ is the Fourier transform of the spherical
top hat window inside which the densities are averaged.

(II.2) Placing particles uniformly inside the box

Obvious approach : Place particles at points of a regular
grid with cell size L/N

However, this introduces grid anisotropies (preferred directions).

Therefore, one often uses "glass"-like pre-initial conditions
(White 1996) : First, place particles randomly inside
the box. Then, evolve particles under a "reversed-sign"
gravitational force. This results in a highly uniform
particle distribution without preferred directions.

Note: One cannot start with particles randomly distributed
in the box. This is because the associated
Poisson-noise would induce spurious nonlinear
evolution.

II.3 Displacing the particles to generate desired $\delta(\vec{x})$

Zeldovich approximation (e.g., Mo, van den Bosch, White 2010)

$\vec{q}$: initial positions, representing uniform density field $\bar{\rho}$

new positions $\vec{x}(t) = \vec{q} + \vec{d}(q,t)$, $\vec{d}$: displacement

The new density field is then given by

$$\rho \, d^3\vec{x} = \bar{\rho} \, d^3q$$

$$\Rightarrow \rho(\vec{x},t) = \bar{\rho} \det\left(\frac{\partial q_i}{\partial x_j}\right)$$

$$= \bar{\rho} \, / \det\left(\frac{\partial x_j}{\partial q_i}\right)$$

$$= \bar{\rho} \, / \det\left(\delta_{ij} + \frac{\partial d_j}{\partial q_i}\right)$$

For small displacements :

$$\left| \delta_{ij} + \frac{\partial d_j}{\partial q_i} \right| \approx 1 + \nabla_q \cdot \vec{d}$$

$$\Rightarrow \delta = \frac{\rho - \bar{\rho}}{\bar{\rho}} = \frac{\bar{\rho}}{(1 + \nabla_q \cdot \vec{d})\bar{\rho}} - \frac{\bar{\rho}}{\bar{\rho}} = \nabla_q \cdot \vec{d}$$

Compare this with linear theory: $\delta(t) = D(t) \, d_0$

$$\Rightarrow \vec{d}(t,q) = D(t) \, \vec{d_0}$$

velocity: $\dot{\vec{x}} = \dot{\vec{d}} = \dot{a} \frac{dD}{da} \vec{d_0} = \frac{\dot{a}}{a} a \frac{dD}{da} \frac{\vec{d}}{D}$

$$\Rightarrow \boxed{\dot{\vec{x}} = H(a) \frac{d \ln D}{d \ln a} \vec{d}} \quad \text{initial particle velocities}$$

Compare with Poisson equation :

$$\left. \begin{array}{l} \nabla^2 \phi' = 4\pi G \, \bar{\rho} \, \delta \\ \delta = \nabla_q \cdot \vec{d} \end{array} \right\} \quad \boxed{\vec{d} = \frac{\nabla \phi'}{4\pi G \, \bar{\rho}}} \quad \begin{array}{l} \text{initial} \\ \text{displacement} \end{array}$$

III.) Gas

The dynamics of the gas is described by the inviscid Euler equations:

$$\frac{d\rho}{dt} + \rho \nabla \cdot \vec{v} = 0 \qquad \text{(mass conservation)} \quad \text{continuity equation}$$

$$\frac{d\vec{v}}{dt} + \frac{\nabla P}{\rho} = 0 \qquad \text{(momentum conservation)}$$

$$\frac{du}{dt} + P \nabla \cdot \vec{v} = 0 \, , \qquad \text{(energy conservation)} \quad \text{internal energy}$$

where

$$\frac{d}{dt} = \frac{\partial}{\partial t} + \vec{v} \cdot \nabla$$

$$\text{E.g.:} \quad \frac{d\rho}{dt} = \frac{\partial \rho}{\partial t} + \vec{v} \cdot \nabla \rho - \rho \nabla \cdot \vec{v} = \frac{\partial \rho}{\partial t} + \vec{\nabla} \cdot (\rho \vec{v})$$

III.1 Discretization

There are two main methods to solve the Euler equations:
  a) Eulerian — the fluid volume is discretized   (cells)
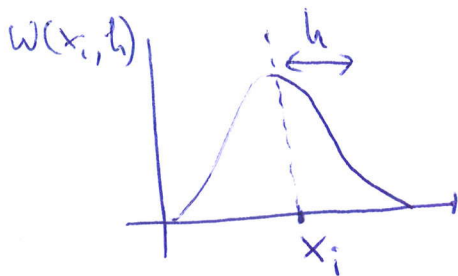 b) Lagrangian — the fluid mass is discretized   (particles)

The Lagrangian approach is intrinsically spatially adaptive: Because fluid elements have constant mass, an increase in density can only be achieved by confining ~~posi~~ these elements in a smaller volume.

Cosmological simulations are characterized by a large dynamic range in density. In this regime, spatially adaptive Lagrangian treatments have been more widely /easily employed than Eulerian treatments. The most widely used incarnation of Lagrangian methods is Smoothed Particle Hydrodynamics.

III. 2 Smoothed Particle Hydrodynamics (SPH)

Lucy (1977), Gingold & Monaghan (1977)

Divide the fluid into particles of mass m. Give each particle a shape, inside which their mass is smoothed out

h: Smoothing (kernel) length

We now derive the equation of motion for these particles. We start with a more general consideration of interpolation:

$$A(\vec{x}) = \int A(\vec{x}') \, W(\vec{x} - \vec{x}') \, d\vec{x}'$$

A: quantity of interest

Discretize:

$$\int d^3\vec{x}' \rightarrow \sum_j \frac{m_j}{\rho_j} \qquad \text{(sum over all particles)}$$

$$\Rightarrow A(\vec{x}) = \sum_j \frac{m_j}{\rho_j} A(\vec{x}_j) \, W(\vec{x} - \vec{x}_j)$$

We can evaluate this at the location of particle i,

$$A_i \equiv A(\vec{x}_i) = \sum_j \frac{m_j}{\rho_j} A_j \, W_{ij}$$
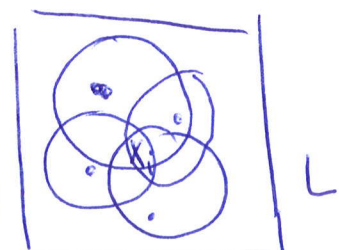
Example: Density

$$\rho_i = \sum_j m_j W_{ij}$$

$W_{ij} = W_{ij}(h_i)$

particle i gathers its mass from particles j

$W_{ij} = W_{ij}(h_j)$

particles j "scatter" their mass to particle i

L

(14)

Note :

Equation for the density replaces the continuity equation,
It needs to be supplemented with an equation for h.
To benefit from the spatial adaptivity, one usually uses

$$h_i \propto \left(\frac{1}{\rho_i}\right)^{1/3}$$

We can also evaluate derivatives directly on the particles :

$$\nabla A(\vec{x}) = \nabla \sum_j \frac{m_j}{\rho_j} A_j \, \omega(\vec{x}-\vec{r}_j)$$

$$= \sum_j \frac{m_j}{\rho_j} A_j \, \nabla W(\vec{x}-x_j)$$

$$\Rightarrow \nabla A_i = \sum_j \frac{m_j}{\rho_j} A_j \, \nabla W_{ij}$$

Note : For simplicity, we have ignored the dependence of
$h = h(\rho(\vec{x}))$ on $\vec{x}$. See III.3 below.

Example : Euler equation

$$\nabla P = \sum \frac{m_j}{\rho_j} P_j \, \nabla W_{ij}$$

Problem : not symmetric (but want "actio = reactio")

Symmetrize : $\nabla P = \frac{1}{\rho}\left[P\nabla\rho - \nabla\rho P\right]$

$$\Rightarrow \nabla P_i = \frac{1}{\rho_i}\left\{P_i \sum_j \frac{m_j}{\rho_j} \rho_j \nabla W_{ij} - \sum \frac{m_j}{\rho_j} \rho_j P_j \nabla W_{ij}\right\}$$

$$= \frac{1}{\rho_i}\left\{\sum m_j (P_i - P_j)\nabla W_{ij}\right\}$$

But we could have also started with

$$\nabla P = \rho\left\{\frac{P}{\rho^2}\nabla\rho + \nabla\frac{P}{\rho}\right\}$$

(15)

then,

$$\nabla P_i = \rho_i \left\{ \frac{P_i}{\rho_i^2} \sum \frac{m_j}{\rho_j} \rho_j \nabla W_{ij} + \sum \frac{m_j}{\rho_j} \frac{P_j}{\rho_j} \nabla W_{ij} \right\}$$

$$= \rho_i \left\{ \sum m_j \left(\frac{P_i}{\rho_i^2} + \frac{P_j}{\rho_j^2} \right) \nabla W_{ij} \right\}$$

⇒ the SPH discretization is not unique. Which one to choose?

→ the natural discretization follows from the Lagrangian (next section)

III.3 Derivation from the Lagrangian

The Lagrangian associated with the Euler equations is (Echart 1960)

$$L = \int \rho \left(\frac{v^2}{2} - u \right) d\vec{x}$$

⇒ SPH discretization (Gingold & Monaghan 1982, Springel & Hernquist 2002, Price 2008)

$$L = \sum_i \frac{1}{2} m_i v_i^2 - m_i u_i$$

The equations of motion are (e.g Landau & Lifshitz 1997)

$$\frac{d}{dt} \left(\frac{\partial L}{\partial \vec{v}_i} \right) - \frac{\partial L}{\partial \vec{r}_i} = 0$$

⇒

$$\frac{\partial L}{\partial \vec{v}_i} = m_i \vec{v}_i$$

$$\frac{\partial L}{\partial \vec{r}_i} = - \sum_j m_j \frac{\partial u_j(\rho_j, s)}{\partial \rho_j} \bigg|_{s_j} \frac{\partial \rho_j}{\partial \vec{r}_i}$$

s: entropy. We have assumed that the fluid flows adiabatically, i.e., $s = $ const. See Sec III 4 below for non-adiabatic flows.

(16)

We also know from the First Law of Thermodynamics:

$$dU = -P dV$$

Therefore, using $V = m/\rho$

$$\frac{\partial u_j}{\partial \rho_j} = \frac{P_j}{\rho_j^2}$$

Finally, using $\rho_j = \sum_k m_k W_{jk}(h_j)$,

$$\frac{\partial \rho_j}{\partial \vec{r}_i} = \sum_k m_k \left\{ \nabla_i W_{jk}(h_j) + \frac{\partial W_{jk}}{\partial h_j} \frac{\partial h_j}{\partial \rho_j} \frac{\partial \rho_j}{\partial \vec{r}_i} \right\}$$

$$\Rightarrow \quad \frac{\partial \rho_j}{\partial \vec{r}_i} = \frac{1}{\Omega_j} \sum_k m_k \nabla_i W_{jk}(h_j) \left(\delta_{ij}^{(k)} - \delta_{ki}^{(k)} \right)$$

$$\Omega_j = 1 - \sum_k m_k \frac{\partial W_{jk}}{\partial h_j} \frac{\partial h_j}{\partial \rho_j} \quad , \quad \delta_{ij}^{(k)} : \text{kronecker delta}$$

Plug all terms into the equation of motion:

$$\frac{d\vec{v}_i}{dt} = \sum_j m_j \left\{ \frac{P_i}{\Omega_i \rho_i^2} \nabla W_{ij}(h_i) + \frac{P_j}{\Omega_j \rho_j^2} \nabla W_{ij}(h_j) \right\}$$

<u>Note</u>: The derivation took into account that $h = h(\vec{x})$. Early SPH implementations ignored this dependence. The result was that either energy was conserved (if the energy equation was solved) or entropy was conserved (if the entropy equation was solved), but not both. The more recent SPH implementations that take the dependence of $h(\vec{x})$ into account ("∇h" terms), conserve simultaneously energy and entropy.
(e.g., Springel & Hernquist 2002)

(17)

(III.4) Shocks

So far we have discussed adiabatic flows. However, to capture shocks, entropy needs to be generated. We therefore introduce the viscous force ("artificial viscosity")

$$\frac{d\bar{v}_i}{dt}\Big|_{visc} = -\sum m_j \Pi_{ij} \nabla_i \overline{W}_{ij} \, ,$$

where $\overline{W}_{ij} = \frac{1}{2}\left[W_{ij}(h_i) + W_{ij}(h_j)\right]$ (symmetrised kernel)

and $(\nabla)\Pi_{ij}$ is a parametrised pressure (force) tuned to yield good shocks in tests.
(see, e.g., Springel 2010 for details)

We now need to compensate the work done by the viscous force in the energy equation:
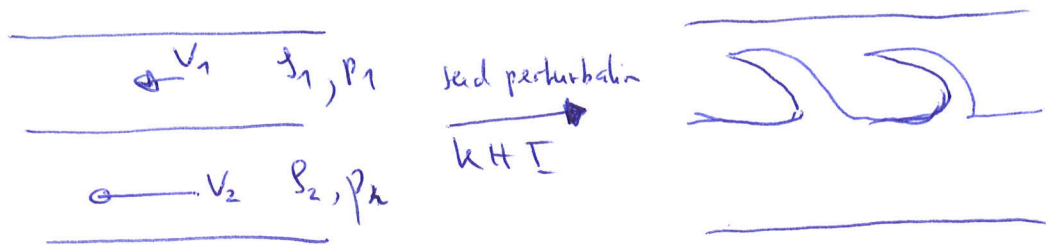
$$\frac{du_i}{dt}\Big|_{visc} = \frac{1}{2}\sum_{j=1} m_j \Pi_{ij} \bar{v}_{ij} \cdot \nabla_i \overline{W}_{ij}$$

<u>Note</u>: The failure to capture shocks without artificial viscosity is not a failure intrinsic to SPH, but to the formulation of the fluid equations. These equations assume that fluid quantities are continuous and can be differentiated. This assumption breaks down at discontinuities such as shocks. The introduction of an artificial viscosity smooths the discontinuities (slightly), such that they can be described by the Euler equations.
→ An alternative would be to consider the integral form of the fluid equations.

(18)

III.5   Two known issues with SPH

a)   Kelvin-Helmholtz instability (KHI)

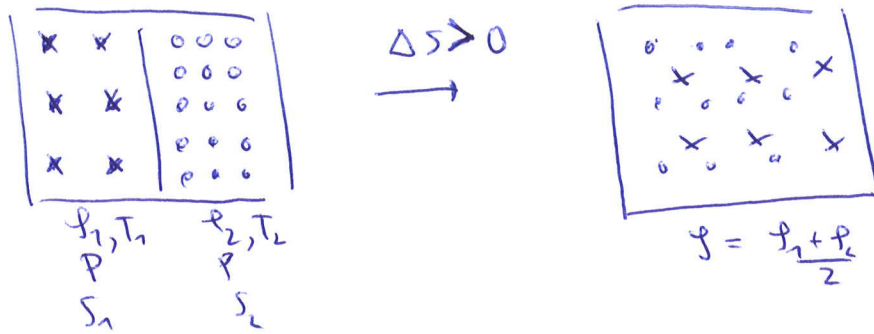at the intersection of two fluids moving with respect to each other (possibly, $\rho_1 = \rho_2$)

In simulations with standard SPH (as explained above), the KHI is suppressed.

Price (2008) has pointed out that this is not a failure of SPH to treat the instability (e.g., the instability develops, if $\rho_1 = \rho_2$), but to treat contact discontinuities, the latter is because of its derivation from differential equations. He shows that SPH can treat KHI also for $\rho_1 \neq \rho_2$ if an artificial conductivity is introduced in the energy equation that smoothes (slightly) the pressure discontinuity at the interface of the two fluids.

b)   Mixing

In the derivation of the SPH equations from a Lagrangian we have assumed that the entropy per particle is constant.

Mixing of fluids requires an increase in entropy:

$$\Delta S > 0$$

$$\rho_1, T_1 \qquad \rho_2, T_2$$
$$P \qquad P$$
$$S_1 \qquad S_2$$

$$\rho = \frac{\rho_1 + \rho_2}{2}$$

Because particle entropies are constant, the total entropy cannot increase. In standard SPH, mixing is therefore energetically forbidden (for details: Springel 2010) The introduction of an artificial conducting could help solving also this problem.

III.6 Comparison with Eulerian method

	SPH	Grid
Advantages:	• Intrinsically spatially adaptive • Galilean invariant • Can model arbitrary geometries • Can be naturally coupled to gravity (N-body)	• high-resolution shock capturing • Entropy generation occurs naturally when matter is mixed in cells
Disadvantages:	• Monte-Carlo-like noise • standard formulation has problems with fluid instabilities & mixing • relatively poor shock resolution • robust	• not adaptive (unless AMR) • not Galilean invariant • preferred directions • resolution (in AMR) increases discontinuously • needs tracer particles to visualize mass flow

⟹ A promising development is the construction of moving mesh codes, which combine the advantages of SPH and Grid (e.g., AREPO, Springel 2009)

(20)